DOI 10.1007/s11182-019-01787-9

Russian Physics Journal, Vol. 62, No. 5, September, 2019 (Russian Original No. 5, May, 2019)

HYDROGEN EFFECT ON THE DEFECT STRUCTURE FORMATION IN THE Zr – 1 WT.% Nb ALLOY UNDER PULSED ELECTRON BEAM IRRADIATION

I. P. Mishin,[1] G. P. Grabovetskaya,[1] E. N. Stepanova,[2] R. S. Laptev,[2] and A. D. Teresov[3]

UDC 539.25:539.1.043:539.26

Using the methods of X-ray structural analysis and electron and positron spectroscopy, it is found out that an irradiation of the surface of a Zr *– 1 wt.%* Nb *specimen with an electron beam in the melting mode results in the formation of lamellar α+α′-structure, an increase in the dislocation density, a dissolution of the β-*Nb *phase, and the formation of defects of the vacancy-impurity type. The presence of hydrogen in the alloy irradiated with an electron beam favors the formation of complex hydrogen-vacancy complexes in the surface layer along with dislocations.*

Keywords: zirconium alloy, hydrogen, pulsed electron beam, defects.

INTRODUCTION

In recent years, in order to improve service characteristics of metallic materials and form protective coatings, their surface is modified by irradiation with electron and ion beams [1, 2]. In the course of electron and ion beam impact on the material, high temperature and stress gradients are formed in the subsurface layers, which results in defect formation [3–8]. These defects interact with those already present in the crystal, which can give rise to new defects [9, 10]. An essential change in the density and type of defects formed by irradiation can be achieved by the presence of hydrogen in the material. It is well known that hydrogen can induce the formation of new defects in material and actively interact with the structure defects already available in it [11–13]. The material stability to hydrogen embrittlement depends on the type and number of the defects present in it. From this perspective, it is important to investigate the influence of hydrogen on the defect structure evolution in the material under its electron beam irradiation.

In this study we perform a comparative investigation of the effect of irradiation with pulsed electron beams on the defect structure of the Zr – 1 wt.% Nb and Zr – 1 wt.% Nb – 0.21 wt.% H alloys.

EXPERIMENTAL MATERIALS AND PROCEDURES

The initial experimental material was a Zr – 1 wt.% Nb zirconium alloy with the hydrogen content 0.0016 wt.% (Zr – 1 Nb alloy in what follows). Hydrogenation of the cylindrical workpieces to a concentration of ~0.21% (here and

[1]Institute of Strength Physics and Materials Science of the Siberian Branch of the Russian Academy of Sciences, Tomsk, Russia, e-mail: mip@ispms.tsc.ru; grabg@ispms.tsc.ru; [2]National Research Tomsk Polytechnic University, Tomsk, Russia, e-mail: enstepanova@tpu.ru; laptev.roman@gmail.com; [3]Institute of High Current Electronics of the Russian Academy of Sciences, Tomsk, Russia, e-mail: tad514@sibmail.com. Translated from Izvestiya Vysshikh Uchebnykh Zavedenii, Fizika, No. 5, pp. 112–117, May, 2019. Original article submitted February 28, 2019; revision submitted April 4, 2019.

further in the text hydrogen concentration is given in wt.%) was performed by annealing in a hydrogen medium at the pressure 1 atm and temperature 873 K in a PCIM high-vacuum device of the Siverst type. After hydrogenation, the workpieces were homogenized at the temperature 853 K for 15 hours. Hydrogen concentration in the ingots was measured using a RHEN 602 gas analyzer accurate to 0.0001%.

Irradiation of the alloy specimens with pulsed electron beams was performed in a SOLO facility equipped with an electron source [14]. Two irradiation regimes were used: melting mode (energy density 12 J/cm^2) and no-melting mode (energy density 5 J/cm^2). In both cases, three pulses were used with the pulse rate 0.3 s^{-1} and pulse duration 50 μs. The specimens measuring 20 mm in diameter and 0.8 mm in thickness were irradiated in an argon atmosphere at a residual pressure of 0.02 Pa. The irradiated surface area was ~2.6 cm^2. Prior to irradiation, the specimen surfaces were mechanically ground and electrolytically polished.

The alloy structure was examined in the optical (AXIOVERT-200MAT) and transmission (JEM-2100) electron microscopes. The structural element dimensions were determined by the secant method in the respective microstructural images. The sampling size was no less than 200 elements.

The dimensions of coherent-scattering regions (D) and the values of crystal lattice microdistortions ($\Delta\varepsilon$) in the alloy were determined by the standard X-ray diffraction methods using a Shimadzu XRD-7000 diffractometer in the CuK_α emission from broadening of the diffraction peaks at their half-height using the Cauchy approximation [15]. The diffraction patterns were interpreted using the PowderCell software. In order to differentiate between the contributions from coherent-scattering regions and lattice microdistortions into the diffraction peak broadening, use is generally made of the maxima belonging to one and the same family of planes. For an HCP-lattice, it is difficult to obtain a second-order maximum. For this reason, we used the diffraction maxima from the (100), (101) and (103) planes. The total dislocation density (ρ) due to the presence of coherently scattering regions and crystal lattice microdistortions was calculated using the following formula [16]:

$$\rho = \left(\rho_1 \rho_2\right)^{1/2} = \left(\frac{3}{D^2} \frac{k\Delta\varepsilon^2}{b^2} \right)^{1/2}, \quad (1)$$

where $\rho_1 = 3/D^2$ is the dislocation density due to the presence of coherently scattering regions, $\rho_2 = k\Delta\varepsilon^2/b^2$ is the dislocation density due to the crystal lattice microdistortions, b is the Burgers vector 1/3[110], and k is the constant related to elastic properties of a material (for zirconium it is ~16).

In order to analyze the prevailing defect types, formed under irradiation with a pulsed electron beam, we used the method of positron spectroscopy. The investigation was performed with a hybrid digital positron-spectroscopy system with an option of external synchronization based on the modules of spectroscopy over the positron annihilation lifetimes (PALS) and coincidence of the Doppler broadening positron annihilation lines (CDBS), which was developed in the Division for Experimental Physics of the TPU [17]. The time resolution of the PALS module is (170 ± 7) ps, the count rate – (90 ± 30) counts/s, the count rate for the CDBS module – (116 ± 15) counts/s for the energy resolution (1.16 ± 0.03) keV. The source of positrons was a ^{44}Ti radioisotope source with the radioactivity 0.91 MBq and maximum positron energy 1.47 MeV. The PALS spectra were processed with an LT10 (ver. 10.2.2.2) software program using a three-component positron trapping model [18]. For the analysis, three-time components were used: τ_1, τ_2, τ_3 with the respective intensities I_1, I_2, I_3. Two dimensional CDBS spectra were processed with the CDBTools. For the analysis, use was made of the traditional S and W CDBS-parameters, characterizing the processes of annihilation of positrons with valence- and core-shell electrons, respectively [18]. It is well known [18] that in the course of the positron trapping by defects (dislocations, vacancies), increasing the free volume, the probability of annihilation of the positrons with the valence electrons, having small momenta, increases, while that with the core-shell electrons, having large momenta, decreases. This gives rise to an increase in the S-parameter and a decrease in the W-parameter. Parameter W is sensitive to the chemical composition in the site of positron annihilation. Its variation indicates the presence of impurity or alloying elements in the site of positron annihilation.

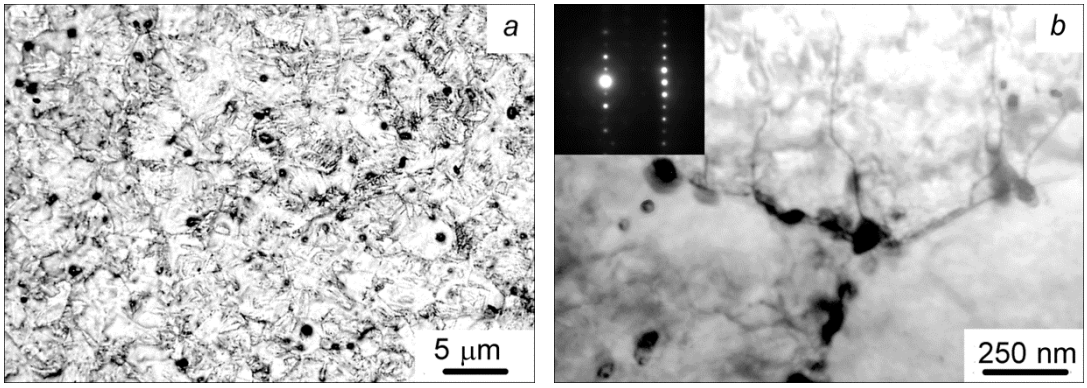

Fig. 1. Microstructure of the Zr – 1 Nb (*a*) and Zr – 1 Nb – 0.21 H (*b*) alloys in the initial state.

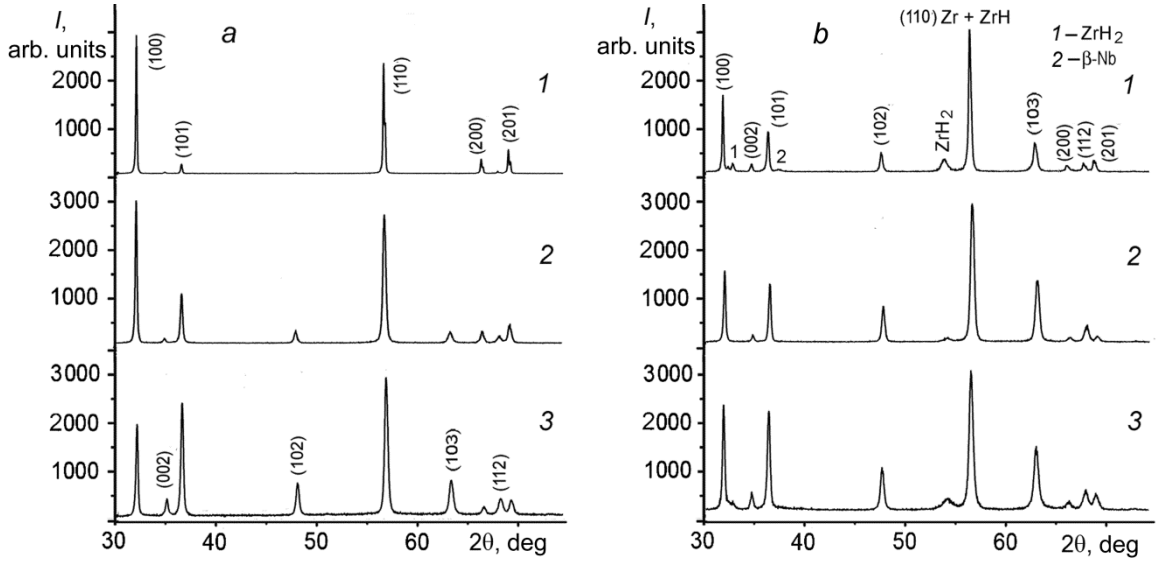

Fig. 2. Sections of diffraction patterns obtained from the Zr – 1 Nb (*a*) and Zr – 1 Nb – 0.21 H (*b*) alloys: curve *1* – initial state, curve *2* – after electron beam irradiation in the no-melting regime, curve *3* – after electron beam irradiation in the melting mode.

RESULTS AND DISCUSSION

The Zr – 1 Nb alloy, used in this study in an as-received state, has a polycrystalline structure with the average grain size 4 μm. In addition to the major α-Zr phase, the alloy contains a small amount of β-Nb phase (Zr solid solution based on Nb). The β-Nb phase in the form of particles, measuring from a few tens of nanometers to a few microns, is present in the bulk of the alloy grains and at the grain boundaries (Fig. 1*a*). The volume fraction of the β-Nb phase determined by the standard grid method from the microstructure images does not exceed 2 vol.%.

The optical- and electron-microscopy structural investigations have demonstrated that hydrogenation of the Zr – 1 Nb to 0.21 wt.% (in what follows Zr – 1 Nb – 0.21 H alloy) changes neither the average grain size nor the volume fraction of the β-Nb particles (Fig. 1*b*). However, according to the X-ray diffraction data, upon hydrogenation of the Zr – 1 Nb – 0.21 H, such hydrides as ZrH and ZrH_2 are observed in it (Fig. 2*a* and *b*, Curves *1*). This is indicated by the

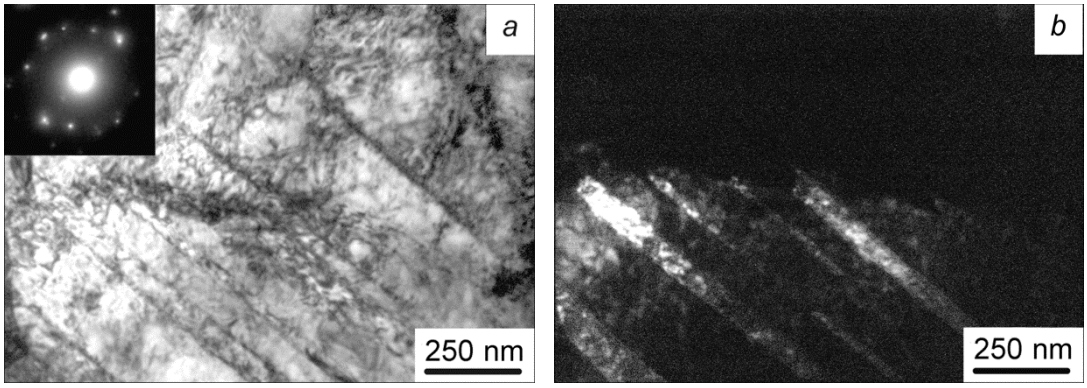

Fig. 3. Microstructure of the subsurface layer of the Zr – 1 Nb – 0.21 H alloy after its irradiation with a pulsed electron beam in the melting mode: *a* – bright-field image and respective microdiffraction pattern, *b* – dark-field image.

(111) and (202) reflections from ZrH zirconium hydride and increased intensity of the (110) reflection from Zr due to overlapping of the (220) reflection from ZrH_2 hydride.

An electron beam irradiation in the no-melting regime does not change either the average grain size or the volume fraction of the β-Nb phase particles in the Zr – 1 Nb and Zr – 1 Nb – 0.21 H alloys. At the same time, the broadening of the X-ray maxima of the α-Zr phase is observed in the X-ray diffraction patterns of both alloys (Fig. 2*a* and *b*, Curves *2*). Note that the ratio of the X-ray peak broadening values is close to the tangent ratio of the respective angles. This indicates a relationship between the X-ray peak broadening and the crystal lattice microdistortion (Δε). The values of Δε from the α-Zr phase, calculated using broadening at half maximum of the X-ray peaks in the initial Zr – 1 Nb and Zr – 1 Nb – 0.21 H alloys are $3.2 \cdot 10^{-4}$ and $1.4 \cdot 10^{-3}$, respectively, and the densities of dislocations chaotically distributed in the grains (ρ) – $1.6 \cdot 10^{13}$ and $3.0 \cdot 10^{14}$ m^{-2}, respectively. After irradiation in the no-melting regime, the values of Δε in α-Zr in the Zr – 1 Nb and Zr – 1 Nb – 0.21 H alloys increase to $1.0 \cdot 10^{-3}$ and $2.1 \cdot 10^{-3}$ respectively, and those of ρ – to $1.5 \cdot 10^{14}$ and $6.7 \cdot 10^{14}$ m^{-2}, respectively. In the bulk of the alloy (~80 μm from the surface) the values of Δε and ρ of in α-Zr hardly change.

As a result of electron beam irradiation in the melting regime, in the surface layer of the alloy 8–10 μm in thickness the average grain size increases from 4 to 6 μm, irrespective of the hydrogen concentration. In the bulk of the grains of this layer a lamellar structure is formed, with the dimensions of the packs of parallel plate being 1–1.5 μm (Fig. 3). The width of the plate in the packs varies from 20 to 300 nm. The plate are observed to contain dislocations. An interpretation of the X-ray diffraction patterns showed that the plate represent α- or α′-phase of zirconium. In the modified layer there are no precipitates of the β-Nb phase. In the bulk of the specimens, there are no changes in the grain size, the volume fraction and the distribution of the β-Nb phase after irradiation of the alloy with a pulsed electron beam in the melting mode.

The form of diffraction patterns obtained from the modified layer (see Fig. 2*a* and *b*, Curves *3*) suggests an increase in the stress in the subsurface layer of the Zr – 1 Nb and Zr – 1 Nb – 0.21 H alloys irradiated in the melting mode compared to the case in the no-melting mode. Note that the ratio of the X-ray peak broadening values lies between the tangent and cosine ratios of the respective angles. This indicates a relationship of the X-ray peak broadening both with Δε and with the real or apparent structure dispersion (coherently scattering regions *D*). According to the estimates made using the Cauchy approximation, the values of *D* in the modified layer of the Zr – 1 Nb and Zr – 1 Nb – 0.21 H alloys are found to be 86 and 58 nm, respectively, and those of Δε – $1.3 \cdot 10^{-3}$ and $2.0 \cdot 10^{-3}$, respectively. The value of ρ, related to Δε, in the Zr – 1 Nb alloy increases to $2.6 \cdot 10^{14}$ m^{-2}, and in the Zr – 1 Nb – 0.21 H alloy it hardly changes ($6.1 \cdot 10^{14}$ m^{-2}). The total values of ρ in the modified layer of the Zr – 1 Nb and Zr – 1 Nb – 0.21 H alloys, which are calculated by formula (1), increase up to $3.2 \cdot 10^{14}$ and $7.4 \cdot 10^{14}$ m^{-2}, respectively. In the bulk of the alloys under study, the values of ρ do not practically differ from their initial values.

TABLE 1. Results of Processing of the Spectra of Time Distribution of Positron Annihilation in the Zr – 1 Nb and Zr – 1 Nb – 0.21 H Alloy Specimens

State	τ_1, ps	I_1,%	τ_2, ps	I_2,%	τ_3, ps	I_3,%
Zr – 1 Nb (CG)	166±1	100	–	–	–	–
Zr – 1 Nb initial FG	166±1	84	215±5	16	–	–
Zr – 1 Nb initial FG after irradiation	166±1	66	193±5	21	320±10	13
Zr – 1 Nb – 0.21 H	166±1	53	205±5	47	–	–
Zr – 1 Nb – 0.21 H after irradiation	166±1	56	209±5	26	280±10	18

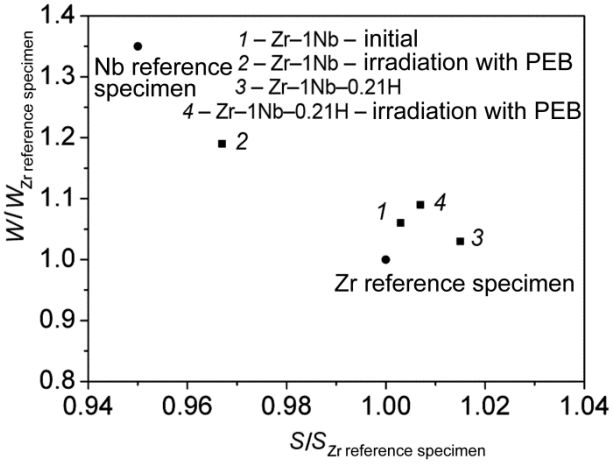

Fig. 4. Interrelation between the parameters of coincidence of the Doppler broadening positron annihilation lines of the Zr – 1 Nb alloy in different states.

A considerably smaller change of the ρ and Δε values in the subsurface layer of the Zr – 1 Nb – 0.21 H after its irradiation compared to that in the Zr – 1 Nb alloy seems to be due to partial hydrogen degassing from this layer during irradiation. This is supported by the results of measurement of the total hydrogen concentration and the X-ray investigations of the surface layer of the Zr – 1 Nb – 0.21 H alloy by the grazing beam method. The total concentration of hydrogen in the alloy irradiated with an electron beam decreases negligibly (by 0.002–0.004 wt.%). Note that there are no hydrides in the surface layer of the ~1 μm-wide Zr – 1 Nb – 0.21 H layer, while they are still observed in the bulk of the alloy.

The results of investigation of the types of defects formed in the modified layer of the Zr – 1 Nb and Zr – 1 Nb – 0.21 H alloys by the method of positron spectroscopy are presented in Table 1 and Fig. 4. It is evident from Table 1 that in the Zr – 1 Nb alloy specimen annealed at 1123 K only one time component, τ_1 = 166 ps, is revealed, which is related to annihilation of positrons from their delocalized states in the zirconium lattice [19]. In the Zr – 1 Nb alloy specimens, used in this study, in addition to the τ_1 component, a long-lived τ_2 = (215±5) ps component is revealed, whose value is consistent with the lifetime of the positrons captured by dislocations in the zirconium alloy [20].

In the Zr – 1Nb irradiated in the melting mode, in addition to the τ_1 = 166 ps component, two more long-lived components are observed: τ_2 = (193 ± 5) ps and τ_3 = (320 ± 10) ps. Note also that according to the CDBS data (Fig. 4) there is a decrease in parameter *S* and an increase in parameter *W*, which is inconsistent with the increased dislocation density in the Zr – 1 Nb after its irradiation. The observed changes in parameters *S* and *W* can, in this case, be related to two factors: defect structure redistribution and changes of the chemical neighborhood in the site of positron annihilation. Relying on the literature data [17, 21], one might assume that the increase in *W* and the decrease in parameter *S* and component τ_2 to (193 ± 5) ps in the Zr – 1 Nb alloy after its irradiation results from an increase in the density of defects of the vacancy–impurity type and a redistribution of the probability of annihilation of the positrons

captured by the dislocations and defects of the vacancy–impurity type. This assumption is indirectly supported by the electron microscopy investigations. It was noted above that after irradiation there is no β-Nb phase in the subsurface layer, which indicates the formation of an oversaturated niobium solution in zirconium as a result of melting and fast crystallization. The presence of the τ_3 = (320±10) ps component could be related to annihilation of positrons trapped by the vacancy complexes. It is known [18] that in this case the lifetime of a positron as a function of the number of vacancies in a complex by 1.8–4.1 factors exceeds τ_1.

In addition to the τ_1 component in the Zr – 1 Nb – 0.21 H alloy, there is a long-lived τ_2 = (205±5) ps component with the intensity 47%. Moreover, according to the CDBS data (Fig. 4), in contrast to the Zr – 1 Nb, parameter *S* increases and parameter *W* decreases; this suggests a larger number of defects increasing the free volume. The value of the τ_2 = (205 ± 5) ps component is close to the lifetime of the positrons trapped by dislocations and to the lifetime of those captured by the hydrogen-vacancy complexes (~200 ps). A comparison of the results obtained with the literature data [7, 17, 20] allows assuming that the τ_2 = (205±5) ps component is a superposition of the contributions from the annihilation of the positrons on dislocations and hydrogen-vacancy complexes.

After irradiation in the melting mode, two long-lived components are observed in the Zr – 1 Nb – 0.21 H alloy: τ_2 = (209 ± 5) ps and τ_3 = (280 ± 10) ps. Furthermore, according to the CDBS data (Fig. 4), parameter *W* increases and parameter *S* decreases, which suggests a change in the chemical neighborhood in the site of positron annihilation. Similarly to the case in the Zr – 1 Nb, this could be due to the dissolution of the β-Nb phase and formation of a solid solution as a result of melting and fast crystallization. The observation of the τ_3 component in the alloy indicates the formation of complex hydrogen-vacancy complexes of the *mV*–*n*H type, where *m* is the number of vacancies per complex and *n* is the number of hydrogen atoms bound to the vacancies [17]. The formation of complex hydrogen-vacancy complexes can give rise to the lower density of simple hydrogen-vacancy complexes and, as a result, to a certain increase in the value of the long-lived τ_2 component and a decrease in its intensity.

CONCLUSION

It has been shown that an irradiation of the Zr – 1 Nb and Zr – 1 Nb – 0.21 H alloy specimens in the no-melting mode does not change the size of the grains and β-Nb precipitates, but results in a larger number of crystal lattice microdistortions of the α-Zr phase and a higher dislocation density in the subsurface layer. As a result of irradiation in the melting mode, in the 8–10 μm-thick subsurface layer of the Zr – 1 Nb and Zr – 1 Nb – 0.21 H alloys a lamellar α+α′-structure with a plate size of 20–300 nm is formed. Along with the higher density of defects (dislocations, vacancies, and vacancy complexes), increasing the free volume, one observes the dissolution of the β-Nb phase and the formation of defects of the vacancy-impurity type in the subsurface layer. The presence of hydrogen during irradiation of the Zr – 1 Nb – 0.21 H alloy with a pulsed electron beam in the melting mode favors the formation of complex hydrogen-vacancy complexes in this layer. It should be added that dislocations remain to be the main type of defects.

This study has been financially supported by the RFBR, Grant No. 18-08-00158 and performed using the facilities of the Tomsk Material Common Use Center of the National Research Tomsk State University.

REFERENCES

1. M. C. Li, S. Z. Hao, H. Wen, and R. F. Huang, Appl. Surf. Sci., **303**, 350–353 (2014).
2. Y. J. Liu, S. J. Li, H. L. Wang, *et al*., Acta Mater., **113**, 56–67 (2016).
3. I. P. Mishin, E. N. Stepanova, G. P. Grabovetskaya, *et al*., Izv. Vyssh. Uchebn. Zaved. Fiz., **55**, No. 12/2, 224–227 (2012).
4. X. D. Zhang, S. Z. Hao, T. Zou, *et al*., J. Metall., **2012**, 762125 (2012).
5. R. Zenker, Adv. Eng. Mater., **6**, 581–588 (2004).
6. J. X. Zou, K. M. Zhang, S. Z. Hao, *et al*., Thin Solid Films, **519**, 1404–1415 (2010).
7. N. S. Pushilina, A. M. Lider, V. N. Kudiyarov, and V. V. Krivosheina, Izv. Vyssh. Uchebn. Zaved. Fiz., **56**, No. 11/3, 57–61 (2013).

8. S. V. Ivanova, Int. J. Hydrog. Energy, **27**, 819–824 (2002).
9. L. D. Panteleev and V. M. Grigoriev, Dimensional Changes in Zirconium and its Alloys under Conditions of Reactor Irradiation. An analytical overview [in Russian], Preprint VNIIMN, Moscow (1976).
10. G. G. Bondarenko, L. N. Bystrov, L. I. Ivanov, and Yu. M. Platov, Usp.Fiz.N auk, **116**, No. 2, 303–314 (1975).
11. J. Cizek, O. Melikhova, and I. Procházka, J. Alloys Compounds, **645**, S312–S315 (2015).
12. P. Hruška, J. Cizek, F. Lukáč, *et al*., Defect and Diffusion Forum, **373**, 122–125 (2016).
13. J. Cizek, I. Prochazka, S. Danis, *et al*., Phys. Rev. B: Condens. Matter, **79**, 054108 (2009).
14. N. N. Koval and Yu. F. Ivanov, Russ. Phys. J., **51**, No. 5, 505–516 (2008).
15. S. S. Gorelik, Yu. A. Skakov, and L. N. Rastorguev, X-Ray Diffraction and Electro-Optical Analysis [in Russian], MISIS, Moscow (2002).
16. G. K. Williamson and R. E. Smallman, Phil. Mag., 1, No, 1 34–46 (1956).
17. A. M. Lider, Positron Spectroscopy for Monitoring Structural Changes in the Metal-Hydrogen Systems, Thesis of Dr. Eng. Sci. 05.11.13, NR TPU, Tomsk (2017).
18. R. Krause-Rehberg and H. S. Leipner, Positron annihilation in semiconductors: Defect studies, Springer Verlag, Berlin, Heidelberg (1999).
19. J. M.C. Robles, E. Ogando, and F. Plazaola, J. Phys. Conf. Ser., **265**, 012006 (2011).
20. P. S. Chowdhury, P. Mukherjee, N. Gayathri, *et al*., Bull. Mater. Sci., **34**, No. 3, 507–513 (2011).
21. T. E.M. Staab, R. Krause-Rehberg, and B. Kieback, J. Mater. Sci., **34**, 3833–3851 (1999).